

Safety of multi-channel stimulation implants: a single blocking capacitor per channel is not sufficient after single-fault failure

Antoine Nonclercq · Laurent Lonys ·
Anne Vanhoestenberghé · Andreas Demosthenous ·
Nick Donaldson

Received: 14 October 2011 / Accepted: 26 February 2012 / Published online: 6 March 2012
© International Federation for Medical and Biological Engineering 2012

Abstract One reason given for placing capacitors in series with stimulation electrodes is that they prevent direct current flow and therefore tissue damage under fault conditions. We show that this is not true for multiplexed multi-channel stimulators with one capacitor per channel. A test bench of two stimulation channels, two stimulation tripoles and a saline bath was used to measure the direct current flowing through the electrodes under two different single fault conditions. The electrodes were passively discharged between stimulation pulses. For the particular condition used (16 mA, 1 ms stimulation pulse at 20 Hz with electrodes placed 5 cm apart), the current ranged from 38 to 326 μA depending on the type of fault. The variation of the fault current with time, stimulation amplitude, stimulation frequency and distance between the electrodes is given. Possible additional methods to improve safety are discussed.

Keywords Blocking capacitor · Electric stimulation · Fault current · Device safety · Tissue damage · Electrodes

1 Introduction

Implanted neuroprostheses allow patients suffering from neural impairments to recover functionality lost as a result of an injury or disease. There are many examples of successful neuroprosthetic devices including cardiac pacemakers, cochlear implants, bladder control implants and dropped foot stimulators. Safety must be assessed before new devices can be tested in patients, even for a pre-commercial trial, in order to obtain regulatory approval, and electrical safety should be given due consideration from the beginning of the electronic design work.

Direct current (DC) flowing through electrodes is a major safety concern, as it may cause tissue damage [10]. For example, it has been reported that DC levels as low as 2–3 μA cause pathological changes in rat spinal cords [10] or in cat auditory nerves [18]. Therefore, both the U.S. Food and Drug Administration (FDA) and E.U. 60601 harmonized standards limit the amount of DC during normal and single fault condition (such as a short-circuit fault in a semiconductor component). For instance, for active implantable medical devices in the E.U., “no leakage current (DC) of more than 1 μA shall be sustained in any of the current pathways when the device is in use” [6]. The mechanisms for stimulation induced tissue damage are not well understood [15]. However, three hypotheses have been proposed: intrinsic biological processes as excitable tissue is over-stimulated (mass action theory) [1], toxic electrochemical reaction products at the electrode surface [3] and electroporation [4]. Total DC is the most usual parameter to draw a safe limit in standards and articles, presumably because this quantity can easily be measured [7]. However, it has been argued that DC density is more likely to be the critical parameter for tissue damage [7, 10], and so some studies rather use it to draw a safe limit (e.g.

A. Nonclercq (✉) · L. Lonys
Biomedical Stimulation and Monitoring Research
Group (BISTIMO), Université Libre de Bruxelles,
Avenue F.D. Roosevelt 50 CP165/51, 1050 Brussels, Belgium
e-mail: anoncler@ulb.ac.be

A. Vanhoestenberghé · N. Donaldson
Implanted Devices Group, Department of Medical Physics
and Bioengineering, Malet Place Engineering Building,
Gower Street, London WC1E 6BT, UK

A. Demosthenous
Department of Electronic and Electrical Engineering,
Malet Place Engineering Building, Gower Street,
London WC1E 6BT, UK

[7, 8]). A simple way to estimate DC density is to divide the DC by the electrode area [10].

A typical way to limit DC is the use of blocking capacitors connected in series with the electrodes. Blocking capacitors have two additional benefits: they ensure that no charge accumulates on the electrodes and they allow “slide back” of the operating potential range of the electrodes so that it tends to remain within the “water window” [5, 12]. When there is only one stimulation channel or when every stimulation channel is electrically isolated by having an independent power supply (as in [2]), the blocking capacitors indeed ensure low levels of DC even during single fault conditions. Usually, however, multi-channel stimulators now use multiplexing and a common power supply (e.g. [12]) so the stimulation channels are not isolated from each other. In that case, despite having blocking capacitors on every channel, there is a possibility that DC may flow between neighbouring channels. This paper explores the effect of short-circuit failures in the stimulator output stage, quantifies the resulting DC and proposes methods of prevention.

2 Methods

A specially-made two-channel stimulator was used to measure DC at the electrodes under short-circuit fault conditions. Each channel was connected to a platinum tripole in the slot of an electrode book [19] immersed in a bath of isotonic saline (9 g of NaCl per liter). The books were placed close together (5 cm apart, unless otherwise noted), corresponding to a worst-case scenario. The area of each anode was 18 mm² and that of each cathode 9 mm². An ammeter (described below) was used to measure DC flowing from and to the electrodes, one at a time. This section describes the circuits used, shows typical waveforms illustrating normal function and describes expected currents under fault condition.

2.1 Stimulator circuit

An output stage of a type used by our team [12] was chosen for this study. It generates a charged-balanced biphasic stimulating current by active charging and floating passive discharge [20]. Figure 1a shows the basic circuit (one channel only). During stimulation, the anode switch (S_a) is closed, the discharge switch (S_d) is open and the current sink (CS) is turned on. During discharge, S_d is closed, S_a is open and the current sink is turned off. The electrodes that are called ‘anode’ (A) and ‘cathode’ (K) are respectively positively and negatively polarized during the stimulation current pulses. A 20 V power supply voltage (V_{dd}), a 2.5 k Ω discharge resistor (R_d) and

a 4.7 μ F blocking capacitor (C_b) were chosen to replicate a typical stimulator. The amplitude of the current sink can be set to 4, 8 or 16 mA (in this paper, an amplitude of 16 mA was used on Ch 1 unless otherwise noted, and it was always 16 mA on Ch 2). The output impedance of the current sink was 134 k Ω when turned on and above 100 M Ω otherwise.

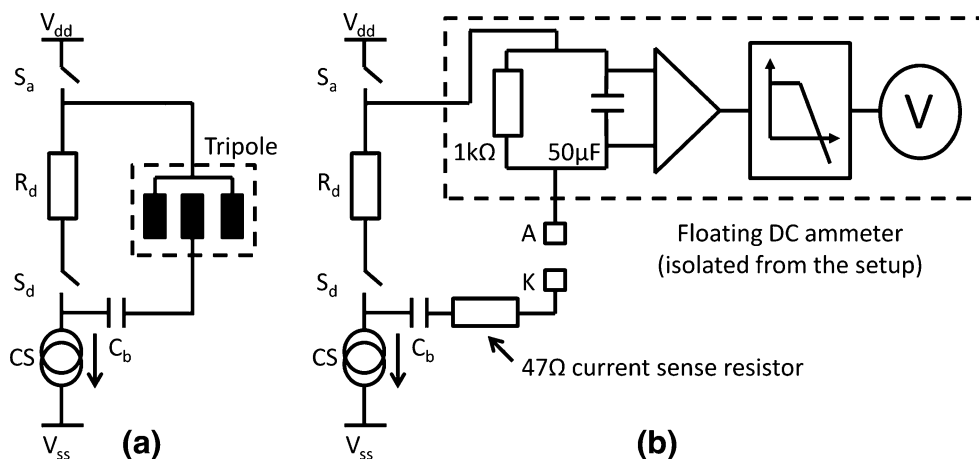
Stimulation pulses were of 1 ms duration and outputs were pulsed alternately at 20 Hz (unless otherwise noted). A microcontroller was used to synchronize both channels: at time t_0 Ch 1 stimulates for 1 ms; at time $t_0 + 25$ ms Ch 2 stimulates for 1 ms; at time $t_0 + 50$ ms the cycle starts again. Manual switches in parallel with the anode switch (S_a) and with the current sink on Ch 2 allow short circuiting one of those components to simulate a fault. Those two faults were identified as the most critical as they link the power rail or the V_{ss} to the electrode (directly or via the blocking capacitor in the case of the current sink).

2.2 DC ammeter

DCs through the electrodes were recorded with an ammeter (Fig. 1b) which was inserted in series with either A_1 or A_2 . The input impedance is formed by a 50 μ F low-leakage polyester capacitor in parallel with a 1 k Ω resistor. The current waveform is low-pass filtered by the combined resistance and capacitance and the DC is the measured average voltage divided by the resistance. The input voltage is buffered by a FET-input instrumentation amplifier (Texas Instruments INA116, with unity gain) with low bias and offset currents (<100 fA) and filtered with a 1 Hz second order low-pass Sallen-Key filter. The output voltage is measured using a digital voltmeter (Fluke 76). The whole system (amplifier, filter and voltmeter) is battery-powered, avoiding this way any connection to mains and therefore minimizing the impact of the ammeter on the setup. The method was adapted from [9, 13]. The ammeter was calibrated (gain and offset) using a linear regression model, obtained by applying known DCs (20 measures, linearly spaced) at its inputs. The average error between the linear regression model and the measures varies from 64 nA for a ± 20 μ A range to 3.3 μ A for a ± 2 mA range. Other combinations of input resistor and amplifier gain allowed lowering the average error between the linear regression model and the measures (down to 70 pA for a ± 10 nA range). In this work, the same measurement setup—and so the same input resistor (1 k Ω)—was used, in order to ensure that the impact of the DC ammeter on the stimulation setup (believed to be small) was also identical for all measures, and so allowing easier comparison.

DCs at the electrodes are measured 60 s after the fault has occurred, leaving time for the stimulating system, the electrodes voltage and the DC measurement to stabilize.

Fig. 1 One stimulation channel. **a** The stimulation tripole is within the slot of a silicone rubber book [12] which is represented by the dashed rectangle. **b** Stimulation channel with the floating DC ammeter



2.3 Typical waveforms

The setup was tested under normal conditions (no fault, all manual switches are open). For each channel, oscilloscope probes were placed at the anode and cathode, and a 47 Ω resistor was placed in series with the blocking capacitor. Current flowing in the cathode was deduced from the voltage drop across the resistor. Figure 2 shows the resulting current and voltage waveforms. When neither tripole is active, the impedance between all of the electrodes and the power rails is very high (above 100 MΩ). The oscilloscope probes have impedance to ground, and when placing the probe on a floating channel, its impedance is placed in parallel to it. Thus, when there is no stimulation, the potentials return to zero pulled down by the probe impedance (1 MΩ in parallel with 95 pF). During stimulation of Ch 1, the active anode voltage is close to the positive supply rail and the cathode potential is determined by the interelectrode impedance (Fig. 2 left). Because Ch 2 is floating at this time, the anode and cathode follow the potential imposed by Ch 1 (between Ch 1 anode and cathode voltages), as seen in Fig. 2 (right). When a channel is discharging, a small discharge current flows from the cathode to the anode, and the potential at the cathode becomes slightly higher than that of the anode. When stimulating with the nominal parameters (electrodes placed 5 cm apart, stimulating at 20 Hz and 16 mA) an average DC of 104 nA was measured with 22 nA standard deviation over 20 measurements. Leakage DC is therefore low under normal conditions.

2.4 Expected currents under fault condition

2.4.1 Current sink failure

Figure 3 explains how current flows during the stimulation and discharge periods of Ch 1. When stimulating, a 16 mA pulse flows from the anode switch (S_{a1}) to the current sink

(S_1), as required. However, because of the short-circuit across S_2 , a large current flows from S_{a1} to the cathode of the faulty channel (K_2) at the same time, charging up the capacitor C_{b2} . This current is determined mainly by the impedance between A_1 and K_2 . A smaller current also flows from A_1 to A_2 and then via S_{d2} to V_{ss} . During the discharge period of Ch 1, Ch 1 is floating so that C_{b2} can only discharge via A_2 . Because an instantaneous fault current flows from A_1 during stimulation but does not come back through it during the discharge period, there is an average current (i.e., DC) flowing at A_1 . The blocking capacitors ensure that DC at the cathodes (K_1 and K_2) is zero. As a result the amount of DC flowing from A_1 equals the amount of DC flowing to A_2 :

$$I_{DC} = \frac{1}{T_{S1} + T_{D1}} \int_{T_{S1}} I_{CS} \cdot dt \tag{1}$$

where,

- I_{DC} is the DC at A_1 or A_2 ,
- T_{S1} is the stimulation period of Ch 1,
- T_{D1} is the discharge period of Ch 1,
- I_{CS} is the current flowing in the current sink of Ch 2.

The fault current is quantified in Eq. (1) for two electrodes. If more than two channels were in use, the fault current would come from more anodes, and hence be greater. During stimulation of Ch 2, the current delivered to its load is too large (above 16 mA) since the current sink is short-circuited. However, since Ch 1 is isolated, no current flows to it. Therefore this large pulse current does not influence the amount of DC (but may still be harmful).

2.4.2 Anode switch failure

Figure 4 shows the current flow during the stimulation and discharge periods of Ch 1 when the anode switch of Ch 2 is shorted. In this fault condition, the current is still controlled

Fig. 2 Current and voltage waveforms during normal operation (no fault) about the time of the stimulating pulse on Ch 1, Ch 2 remains in its discharging state in this period. *Left:* measured current at K₁ and voltages at the electrodes on Ch 1. *Right:* measured current at K₂ and voltages at the electrodes on Ch 2

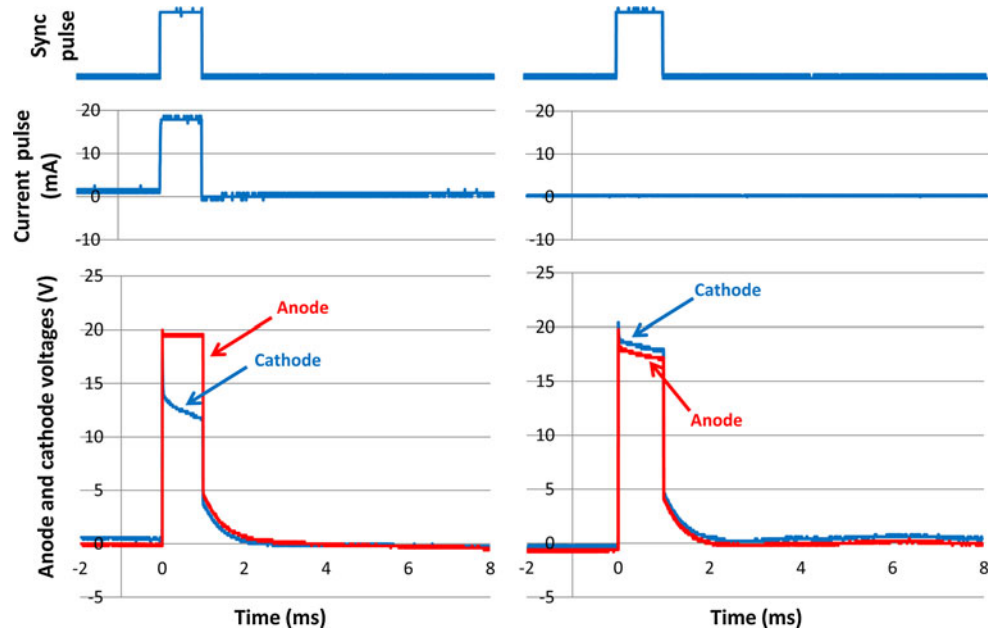
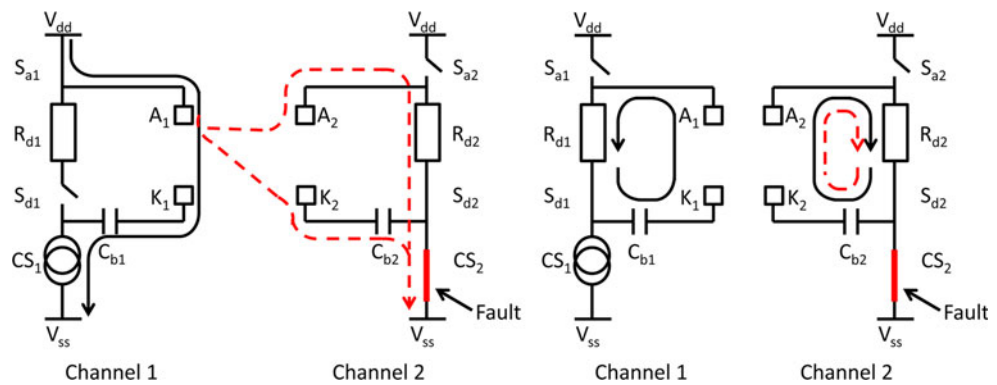


Fig. 3 Current sink failure: current flowing during Ch 1 stimulation (*left*) and discharge (*right*). Currents expected under normal conditions are shown with *plain lines* and currents due to the fault are shown with *dashed lines*



by the current sink of the active channel (CS₁). However that current is now drawn from both anodes. During the discharge time, K₁ and C_{b1} can only discharge through A₁. Because an instantaneous fault current flows from A₂ during stimulation but does not come back through it during the discharge period, there is an average current (i.e., DC) flowing at A₂. Again, the blocking capacitors ensure that DC at the cathodes (K₁ and K₂) is zero and as a result the amount of DC flowing from A₂ equals the amount of DC flowing to A₁:

$$I_{DC} = \frac{1}{T_{S1} + T_{D1}} \int_{T_{S1}} I_{Sa} \cdot dt \tag{2}$$

where I_{Sa} is the current flowing in the shorted anode switch of Ch 2; all the other terms are identical to the ones of Eq. (1). Note that, compared with the current sink fault the net DC now flows in the opposite direction.

3 Results

This section compares the system under normal then single fault condition, respectively for a current sink short-circuit then an anode switch (S_a) short-circuit in Ch 2.

3.1 Current sink failure

Figure 5 shows the resulting current and voltage waveforms. In Ch 1 (left of the figure) the voltage drop between the anode and cathode is larger than in Fig. 2 because more than 16 mA flows from the active anode. A current pulse is now seen on Ch 2 (right of the figure). Ch 2 anode and cathode are connected to V_{ss} (through the blocking capacitor for K₂ and the discharge resistor for A₂).

When stimulating with the nominal parameters (electrodes placed 5 cm apart, stimulating at 20 Hz and 16 mA) an average DC of 326 μA was measured with 2.26 μA

Fig. 4 Anode switch failure: current flowing during Ch 1 stimulation (left) and discharge (right). Currents expected under normal conditions are shown with plain lines and currents due to the fault are shown with dashed lines

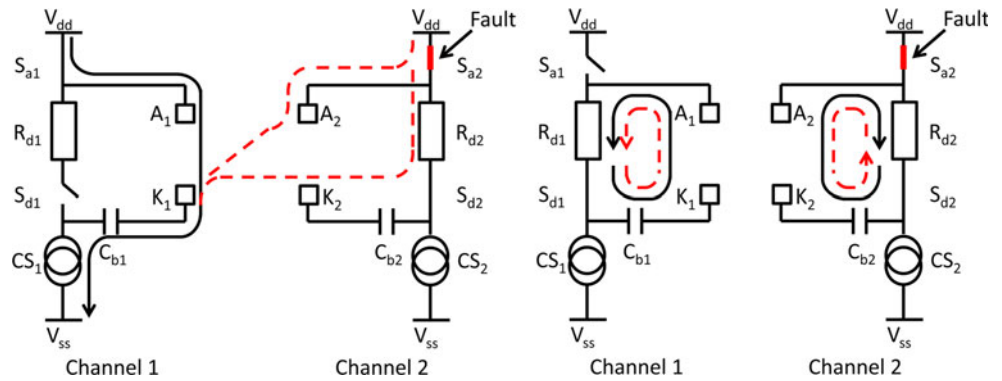
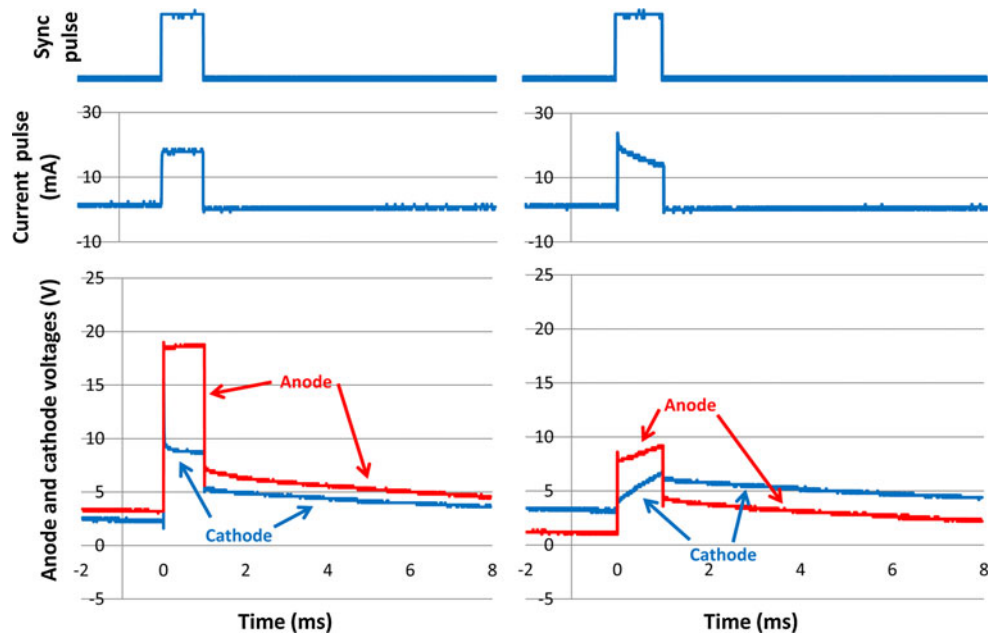


Fig. 5 Current and voltage waveforms during current sink failure. Format same as Fig. 2



standard deviation over 20 measurements. Identical readings were taken from both anodes (A₁ and A₂), as expected (in the following, the measurements were taken at A₂). Variations of the DC with time, stimulation amplitude, stimulation frequency and distance between the electrodes are shown in Fig. 6.

The measured DC fluctuates in a repeatable fashion over time (Fig. 6a): slow decreases are followed by sudden increases. The slow decreases are due to bubbles forming over the electrode surface as a result of electrolysis. Periodically these float away (the arrows indicate each time a bubble came off), freeing the electrode surface, hence lowering the impedance and causing the jump in measured current. In this paper, the measurements are taken 60 s after initiating the fault to ensure a good reproducibility, because bubbles took much longer to form.

The DC decreases as the pulse amplitude of Ch 1 (with intact current sink) increases (Fig. 6b). The fault current flows from A₁ to the lower power rail via the shorted current sink of Ch 2. It is determined by the voltages at

the electrodes of Ch 2 (A₂ and K₂). The voltage at A₂ is equal to V_{dd} minus the voltage dropped from A₁ to A₂ at the electrodes and through the saline. Similarly, the voltage at K₂ is equal to V_{dd} minus the voltage dropped from A₁ to K₂ at the electrodes and through the saline. During the stimulation pulse, the higher the stimulation current, the higher the voltage drops from A₁ to both electrodes of Ch 2, the lower the fault current to the shorted current sink (CS₂). The linear shape of the curve suggests that the impedance of the electrode and the solution is constant with current amplitude in the considered range.

The variation with stimulation frequency shows a linear behaviour at low frequency, with saturation at higher frequencies (Fig. 6c). From Eq. (1), if I_{CS} were constant, the DC variation with stimulation frequency should be linear, since the stimulation frequency is equal to 1/(T_{S1} + T_{D1}). However, as the frequency increases, the blocking capacitor of the second channel does not have time to fully discharge and the fault current tends to saturate.

Fig. 6 Current sink failure: variation of the DC with time (top left), stimulation amplitude (top right), stimulation frequency (bottom left) and distance (bottom right)

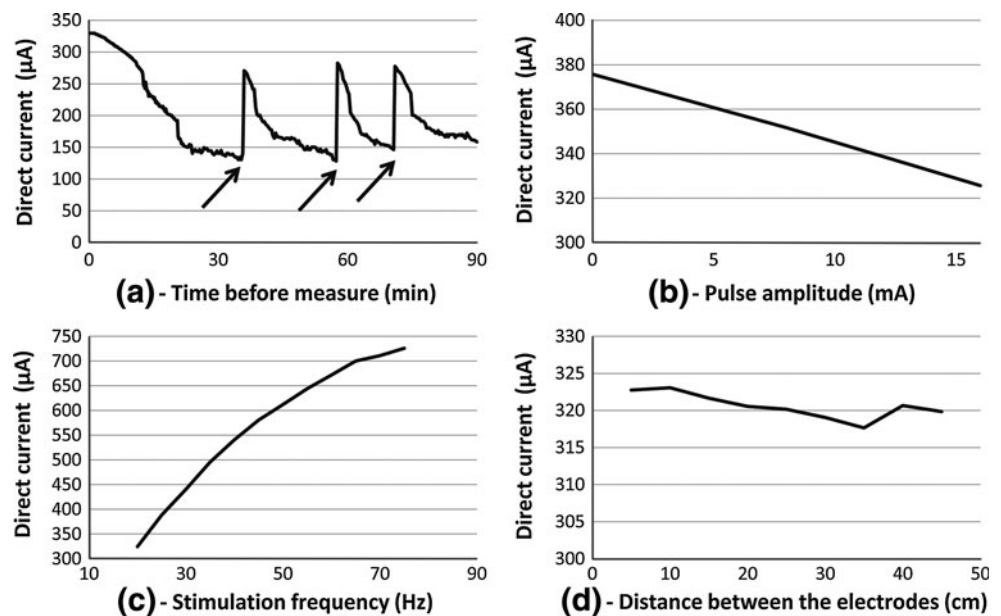
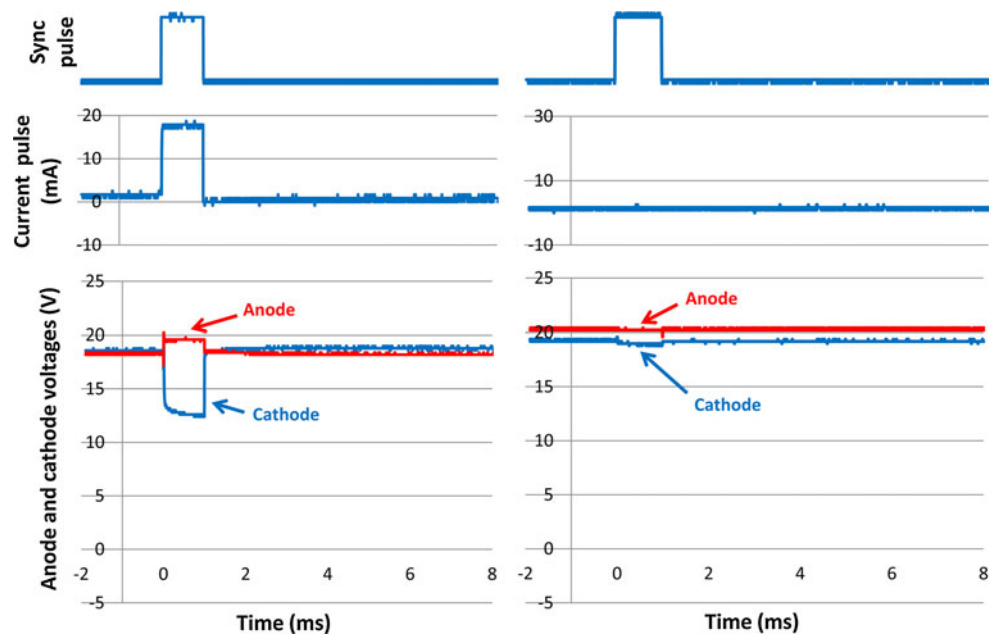


Fig. 7 Current and voltage waveforms during anode switch failure. Format same as Fig. 2



The variation with the distance between the electrodes did not show any clear trend (Fig. 6d). This limited influence is expected as the solution has a relatively high conductivity and most of the voltage drop is likely to occur at the electrode interfaces and in the slots of the books.

3.2 Anode switch failure

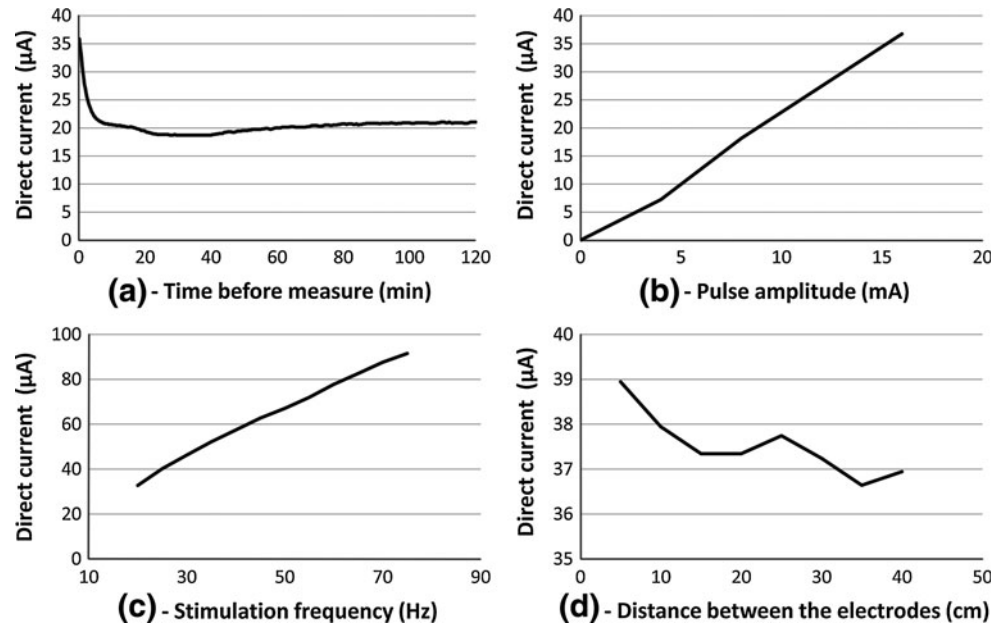
Figure 7 shows the resulting current and voltage waveforms. The potential of the solution is pulled up to the power supply voltage since the anode of the second channel is connected to V_{dd} . Thus, when a channel is

floating, both its electrodes are pulled up to that voltage. When Ch 1 is stimulating, a voltage drop is present between its anode and cathode (Fig. 7 left), because the stimulation current flows between them.

When stimulating with the nominal parameters (electrodes placed 5 cm apart, stimulating at 20 Hz and 16 mA) an average DC of 37.9 μA was measured with 0.57 μA standard deviation over 20 measurements. Variation of the DC with time, stimulation amplitude, stimulation frequency and distance between the electrodes is shown in Fig. 8.

Once the fault is established, the DC decreases and tends to stabilize after about 90 min (Fig. 8a). Here, electrolysis

Fig. 8 Anode switch failure: variation of the DC with time (top left), stimulation amplitude (top right), stimulation frequency (bottom left) and distance (bottom right)



also occurs at the interface, but as the DC level is lower, smaller bubbles form which tend to come off more easily, so that equilibrium between bubble formation and detachment is quicker.

The DC increases as the pulse amplitude of Ch 1 (with intact anode switch) increases (Fig. 8b). This should be expected since the fault current is determined by the amplitude of the current sink of the first channel (CS_1) where it flows. The portion of current flowing into CS_1 from each anode is determined by the impedance of the electrodes and solution. The linear shape of the curve suggests that it is constant with current amplitude in the considered range (similarly to what was observed in the case of current sink failure).

The variation with stimulation frequency shows quite a linear behaviour (Fig. 8c). From Eq. (1), this linear trend implies that the integral of I_{Sa} is constant with frequency, since stimulation frequency is equal to $1/(T_{S1} + T_{D1})$. As I_{Sa} is determined by the potential at A_2 (kept constant at V_{dd}), the current pulse amplitude (kept constant), and the impedance of the electrode and of the solution, it suggests that these impedances are relatively constant with frequency in the range considered.

The variation with the distance between the electrodes did not show any clear trend (Fig. 8d). Again, this limited influence is expected as the solution has a relatively high conductivity and most of the voltage drop is likely to occur at the electrode interfaces and in the slots.

4 Discussion

The result of this study demonstrate that DCs may flow between the anodes in case of an anode switch failure—and

more so in case of a current sink failure—even when using blocking capacitors at the cathodes. The DC is highly dependent on time, stimulation amplitude, and stimulation frequency but not significantly on the distance between the electrodes. These levels of DC would most certainly lead to tissue damage as they are typically one or two orders of magnitude higher than the 2–3 μA level for which damage has already been seen [10, 18].

As DC flows from one anode to the other, maximum DC density may be estimated by dividing the current by the anode area (adapting the method from [10]). For instance, when stimulating with the nominal parameters (electrodes placed 5 cm apart, stimulating at 20 Hz and 16 mA) the DC density is equal to 18.1 $\mu\text{A}/\text{mm}^2$ (326 $\mu\text{A}/18 \text{ mm}^2$) during current sink failure and to 2.1 $\mu\text{A}/\text{mm}^2$ (37.9 $\mu\text{A}/18 \text{ mm}^2$) during anode switch failure. For comparison, using the same estimation, a DC density of 1.5 $\mu\text{A}/\text{mm}^2$ (3 $\mu\text{A}/2 \text{ mm}^2$) causes pathological changes in rat spinal cords [10]. Measured DC densities during those faults are therefore also above—but closer to—the limit for which tissue damage has been reported.

One way to avoid DC for both types of faults would be to add anode blocking capacitors for every channel. However, the extra space this will require is very disadvantageous. A second way would be to use multichannel systems formed from isolated single channels, as is the case for the BION [11, 14]. This approach may be attractive when there are several widely-separated stimulation sites or for systems requiring only few channels. However, it would be unsuitable for a large number of electrodes physically close to one another. A third way would be to monitor the voltage at a node of the circuit that is normally floating when the channel is isolated (e.g. the anode). A short-circuit on the

current sink would be detected as the anode voltage would sink below a pre-agreed threshold during adjacent channel stimulation (because the anode would be pulled down by the short-circuit). Similarly, a short-circuit on the anode switch would be detected as the anode voltage would be constantly at V_{dd} . The difficulty with this would be the arbitrariness of any criterion used, given the undefined potential when there is no fault. A fourth way would be to monitor the voltage drop across the load, to estimate the current flowing in it and by this way ensure it is close to zero when not stimulating, as previously proposed [16, 17]. This monitoring would require a differential amplifier [12], but would greatly increase the complexity of the circuit.

An alternative for current sink failure would be to monitor the current effectively drawn by the circuit by adding a current monitor at the power supply (common to all output stages). If the current drawn exceeds the current defined by the current sink by more than a small amount, a fault is detected and the implant deemed hazardous and switched off. A similar implementation has been previously proposed [16]. Regarding anode switch failure, independent switches at the anode (i.e., redundancy), as well as regular verification of the proper functioning of those switches would ensure the safety of the system.

Other types of failure than those proposed in this paper should also be assessed. For instance, a short circuit in the blocking capacitor might lead to high levels of DC. When blocking capacitors are not integrated, as is usually the case today, this type of failure is unlikely to occur. However, there have recently been developments to integrate blocking capacitors so as to reduce implant size [13] and these capacitors may be less reliable.

In conclusion, the use of single blocking capacitors in each stage of a multiplexed stimulator does not ensure that DC will not flow under single fault conditions. In fact with a plausible stimulation set-up, we demonstrate that the fault current can be large enough to be dangerous. Future designs could take advantage of the present study to enhance their safety.

Acknowledgments The authors thank Prof. Stéphane Godet and Benoit Haut for their help on this study.

References

1. Agnew WF, McCreery DB, Yuen TG, Bullara LA (1993) MK-801 protects against neuronal injury induced by electrical stimulation. *Neuroscience* 52(1):45–53
2. Brindley GS, Polkey CE, Rushton DN (1982) Sacral anterior root stimulators for bladder control in paraplegia. *Paraplegia* 20(6):365–381
3. Brummer S, Turner M (1975) Electrical stimulation of the nervous system: the principle of safe charge injection with noble metal electrodes. *Bioelectrochem Bioenerg* 2(1):13–25
4. Butterwick A, Vankov A, Huie P, Freyvert Y, Palanker D (2007) Tissue damage by pulsed electrical stimulation. *IEEE Trans Biomed Eng* 54(12):2261–2267
5. Donaldson N, Donaldson PEK (1986) When are actively balanced biphasic ('Lilly') stimulating pulses necessary in a neurological prosthesis? II pH changes; noxious products; electrode corrosion; discussion. *Med Biol Eng Comput* 24(1):50–56
6. European Standard (1998) EN45502-1 for safety, marking and information to be provided by the manufacturer in Active Implantable Medical Devices. CENELEC, Brussels, p 8
7. Gilad O, Horesh L, Holder DS (2007) Design of electrodes and current limits for low frequency electrical impedance tomography of the brain. *Med Biol Eng Comput* 45(7):621–633
8. Hernández-Labrado GR, Polo JL, López-Dolado E, Collazos-Castro JE (2011) Spinal cord direct current stimulation: finite element analysis of the electric field and current density. *Med Biol Eng Comput* 49(4):417–429
9. Huang CQ, Shepherd RK, Carter PM, Seligman PM, Tabor B (1999) Electrical stimulation of the auditory nerve: direct current measurement in vivo. *IEEE Trans Biomed Eng* 46(4):461–470
10. Hurlbert RJ, Tator CH, Theriault E (1993) Dose-response study of the pathological effects of chronically applied direct current stimulation on the normal rat spinal cord. *J Neurosurg* 79(6):905–916
11. Kane MJ, Breen PP, Quondamatteo F, ÓLaighin G (2011) BION microstimulators: a case study in the engineering of an electronic implantable medical device. *Med Eng Phys* 33(1):7–16
12. Langlois PJ, Demosthenous A, Pachnis I, Donaldson N (2010) High-power integrated stimulator output stages with floating discharge over a wide voltage range for nerve stimulation. *IEEE Trans Biomed Circuits Syst* 4(1):39–48
13. Liu X, Demosthenous A, Donaldson N (2008) An integrated implantable stimulator that is fail-safe without off-chip blocking-capacitors. *IEEE Trans Biomed Circuits Syst* 2(3):231–244
14. Loeb GE, Peck RA, Moore WH, Hood K (2001) BION system for distributed neural prosthetic interfaces. *Med Eng Phys* 23(1):9–18
15. Merrill DR, Bikson M, Jefferys JGR (2005) Electrical stimulation of excitable tissue: design of efficacious and safe protocols. *J Neurosci Methods* 141(2):171–198
16. Ortmanns M, Rocke A, Gehrke M, Tiedtke H-J (2007) A 232-channel epiretinal stimulator ASIC. *IEEE J Solid-State Circuits* 42(12):2946–2959
17. Schuettler M, Franke M, Krueger TB, Stieglitz T (2008) A voltage-controlled current source with regulated electrode bias-voltage for safe neural stimulation. *J Neurosci Methods* 171(2):248–252
18. Shepherd RK, Linahan N, Xu J, Clark GM, Araki S (1999) Chronic electrical stimulation of the auditory nerve using non-charge-balanced stimuli. *Acta Otolaryngol* 119(6):674–684
19. Tripolar book electrodes, Finetech Medical Ltd, 13 Tewin Court, Welwyn Garden City, Hertfordshire, AL7 1AU, United Kingdom
20. Vanhoestenbergh A (2007) Implanted devices: improved methods for nerve root stimulation. PhD Thesis, University College London, London, United Kingdom